OPEN ACCESS
JOURNAL OF ADVANCED DIELECTRICS
Vol. 12, No. 1 (2022) 2160020 (7 pages)

DOI: 10.1142/S2010135X21600201

Synthesis of ZnO nanorods for piezoelectric resonators and sensors

A. L. Nikolaev*,¶, M. A. Kazmina†, N. V. Lyanguzov‡,
K. G. Abdulvakhidov§ and E. M. Kaidashev†

*Research and Education Center "Materials"
Don State Technical University
No. 1 Gagarin sq., Rostov-on-Don, 344000, Russia

†Vorovich Mathematics
Mechanics and Computer Sciences Institute
Southern Federal University
No. 200/1 Stachki Str. Rostov-on-Don, 344090, Russia

‡Southern Research Center RAS, No. 41 Chehova Str.
Rostov-on-Don, 344006, Russia

§The Smart Materials Research Institute
Southern Federal University
No. 178/24 Sladkova Str. Rostov-on-Don, 344090, Russia

¶andreynicolaev@eurosites.ru

Received 14 April 2021; Revised 7 June 2021; Accepted 8 June 2021; Published 6 October 2021

Efficiency of the piezoelectric chemisensors may be considerably enhanced by use of zinc oxide nanorods as sensing elements. ZnO nanorod arrays being good piezoelectric materials possess large surface area, which provides extra benefits for chemisorption and photodetection. Highly oriented nanorod arrays are typically prepared onto highly crystalline substrates, whereas the nanorods growth onto metal contacts meets significant technological difficulties. In this paper, we report on carbothermal, electrochemical, and hydrothermal techniques of ZnO nanorod arrays synthesis on metal contacts. The optical and structural properties of the obtained nanorods were studied using scanning electron microscopy, X-ray diffraction (XRD), Raman spectroscopy, and luminescence spectroscopy. A reliable technique was developed for obtaining ohmic contact with the grown nanorods. I–U curves of prepared contact were studied. Carbothermal synthesis made it possible to obtain the most crystallinely perfect, homogeneous, and dense arrays of nanorods and control the concentration of point defects by changing the synthesis parameters over a wide range. The electrochemical synthesis demonstrated excellent results for synthesis of ZnO nanorods on the surface of resonator electrodes.

Keywords: Hydrothermal synthesis; electrochemical synthesis; carbothermal synthesis; upper contact; ZnO; nanorods.

1. Introduction

Zinc oxide is a promising semiconducting and piezoelectric material with direct wide bandgap (3.37 eV at room temperature) and large exciton binding energy (60 meV). During the last years, one-dimension nanocrystalline structures such as nanowire, nanorods, nanobelts, and nanocables attract much attention of various research groups[1,2] due to their unique physical properties and potential applications in nanoscale devices. Of particular interest are well-oriented arrays of ZnO nanorods in connection with the combination of excellent electronic and optoelectronic properties of each nanorod. These ZnO nanorods arrays can be used as elements of sensors, actuators, displays and other elements of NEMS as catalysts,[3] etc. New types of efficient piezoelectric chemosensors, ultraviolet (UV) and infrared (IR) photo-detectors based on ZnO bulk acoustic resonators were reported recently.[4–6] In particular, piezoelectric detectors of mass based on bulk resonators with GHz frequency are capable to detect chemical and biological species with sensitivity of ~9000 Hz cm^2/ng.[4] Demonstrated UV photo-detector based on the capacity change of a Schottky barrier built in the bulk acoustic resonator and IR photo-detector based on the temperature-dependent Young's modulus of the resonator material (ZnO) present a new approach to constructing of photoelectric devices.[5–7]

The degree of sensitivity to a certain type of radiation, or a change of bulk resonator condition is expressed by the shift of resonant frequency. The resonance frequency of the bulk resonator can be varied within wide limits because it depends directly on the material of contacts, their mass, geometry, and dimensions.[8] Thus, bulk resonators based on ZnO are a flexible

¶Corresponding author.

tool of modern sensor technology. The ability to change the geometry and characteristics of resonator sensors creates the potential for broad range of detection effects. As an active element of such devices are used nanobelts, thin films, and ZnO nanorods with 753 MHz, 1.6 GHz, and 3.9 GHz resonant frequencies, respectively.[9] As the upper contact Au, Pt, Al films, and Au coated zinc oxide nanorods[10] are typically used. Other designs of resonator sensors are also possible, such as microbalance resonators proven as a high sensitive devices.[11]

Efficiency of these devices may be considerably enhanced by using zinc oxide nanorods as sensing elements. ZnO nanorod arrays being good piezoelectric materials have large surface area, which provides extra benefits for chemisorption. Highly oriented nanorod arrays are typically prepared onto crystalline substrates, whereas the nanorods growth onto metal contacts meets significant technological difficulties. However, the growth of the nanorods on the metal electrodes is ultimately necessary to merge the benefits of high frequency bulk acoustic resonator and nanorod arrays in one device.

A good electrical contact to the nanorod array is also crucial for many devices; however, the design of such contact remains challenging. To enhance the performance of many chemosensors and green/IR photo-detectors, a high concentration of oxygen defects on the surface of ZnO nanostructures is required.

In the present paper, we study the capability of three methods, namely a hydrothermal, electrochemical, and carbothermal synthesis, to obtain a highly oriented nanorod arrays on the top electrode of a bulk acoustic resonator and report a new lift-off procedure to prepare a top Au contact. We also characterize structural, photoluminescent, and lattice vibration properties of the designed structures.

2. Hydrothermal Synthesis

Zinc oxide nanorods were grown on Ag and Au electrodes by hydrothermal synthesis based on the formation and further decomposition of ammonia and hydroxyl complexes of zinc similar to procedure used in Refs. 12 and 13. The prepared sample was mounted vertically in a glass reactor with mixture of 10 mM zinc nitrate hexahydrate and 10 mM hexamine in water bath, heated up to the synthesis temperature of 90 °C, and held at these conditions for 6 h. The chemical processes, which occur on the electrodes surface, can be shortly described by the following reaction chain:

$$\begin{aligned}
&C_6H_{12}N_4 + 6H_2O \rightleftharpoons 6CH_2O + 4NH_3\\
&NH_3 + H_2O \rightleftharpoons NH_4^+ + OH^-\\
&Zn(NO_3)_2 \rightarrow Zn^{2+} + 2NO_3^-\\
&Zn^{2+} + 4NH_3 \rightarrow Zn(NH_3)_4^{2+}\\
&Zn^{2+} + 4OH^- \rightarrow Zn(OH)_4^{2-}\\
&Zn(NH_3)_4^{2+} + 2OH^- \rightarrow ZnO + 4NH_3 + H_2O\\
&Zn(OH)_4^{2-} \rightarrow ZnO + H_2O + 2OH^-
\end{aligned} \tag{1}$$

To improve the quality and the vertical orientation of the nanorods, we prepared nucleation centers by the thermal decomposition of the fine crystals of zinc acetate on the sample surface before the nanorods growth procedure according to the following scheme:

$$\begin{aligned}
&Zn_4O(CH_3COO)_6 \xrightarrow{t^\circ} 4ZnO + 3CH_3COCH_3 + 3CO_2\\
&4Zn(CH_3COO)_2 \cdot 2H_2O \xrightarrow{t^\circ} Zn_4O(CH_3COO)_6\\
&\qquad + (CH_3CO)_2O + 2H_2O
\end{aligned} \tag{2}$$

The length and diameter of the obtained nanorods was about 0.5–2 μm and 30–60 nm, respectively. The advantages of this method are the low synthesis temperature, the availability of reagents, and ease of implementation.

3. Electrochemical Synthesis

The electrochemical synthesis was carried out in the potentiostatic mode at stabilized temperature of 70 °C in a three-electrode cell by using IPC-compact 2000 potentiostat. The scheme of the used setup is shown in Fig. 1.

ZnO nanorod arrays were deposited on Ag or Au contact pads of the bulk quartz resonator. A platinum spiral electrode was used as a counter. The working mixture was a water solution of zinc nitrate hexahydrate and potassium chloride, as a precursor and supporting electrolite, respectively. The potential of -1.1 ± 0.02 V with respect to Ag/AgCl reference electrode was maintained for 3 h. The method can be described by reactions:

$$\begin{aligned}
&NO_3^- + H_2O + 2e^- \rightarrow NO_2^- + 4OH^-\\
&Zn^{2+} + 2OH^- \rightarrow Zn(OH)_2 \xrightarrow{t^\circ} ZnO + H_2O.
\end{aligned} \tag{3}$$

The presence of redox process and precipitation in an electric field produce homogeneous and ordered nano- and micro-objects with high allocation density on the surface, as well as to reduce the growth time in 2–3 times in comparison with the hydrothermal synthesis. The method is highly sensitive to the parameters of the experiment, which creates the possibility of varying the properties of the structures. SEM is a typical technique for studying surface microgeometry

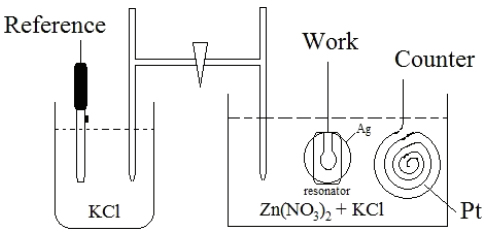

Fig. 1. Scheme of the electrochemical cell used for growth of ZnO nanorod arrays.

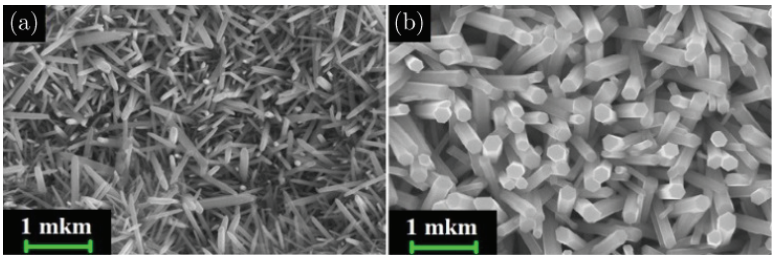

Fig. 2. SEM images of nanorods obtained by hydrothermal (a) and electrochemical (b) methods on Au electrodes, respectively.

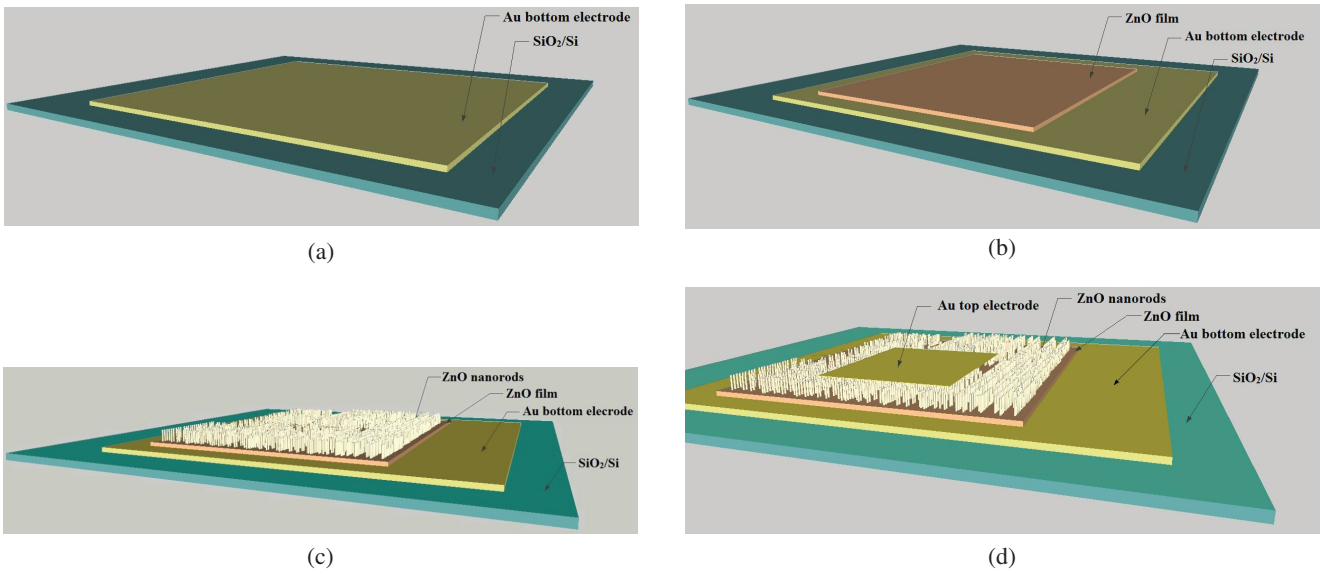

Fig. 3. Scheme of the designed structure with Au bottom and upper electrodes.

of objects in nanoscale.[14–16] The nanorod arrays obtained by hydrothermal and electrochemical synthesis are shown in Fig. 2.

4. Carbothermal Synthesis and Design of the Upper Gold Contact Pad

A thick gold film (~300 nm) was deposited on a cleaned oxidized silicon wafer by pulsed laser deposition (PLD). Then ZnO layer was deposited by PLD onto gold electrode using a mask as it is shown in Fig. 3. Afterwards, the gold nanoparticle array (catalyst) was deposited on the surface of zinc oxide by PLD without changing the mask. An array of ZnO nanorods was grown by carbothermal technique in a setup with quartz tube reactor in the furnace described elsewhere.[17,18] A ZnO:C tablet with molar ratio of 1:1 and a substrate were positioned in a furnace and argon flow of 200 sccm at pressure of 20 mbar was introduced. The reactor was heated up to a synthesis temperature of 1000 °C and the nanorods array was grown for 20 min. Afterwards, the substrate was cooled down to room temperature in argon flow.

The electrodon the top of nanorods array was designed by lift-off technique by the usage of the following steps. A gold film was deposited onto a soluble substrate (NaCl) by PLD method. The film was covered by a thick photoresist layer. Upon dissolving a substrate in water, a gold film was

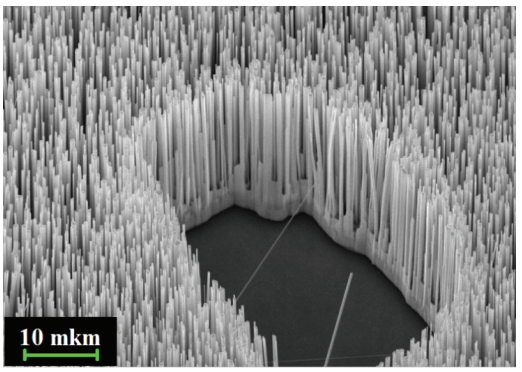

Fig. 4. SEM image of nanorods obtained by carbothermal synthesis on the Au electrode.

positioned on the top of the nanorod array [Fig. 3(d)]. Then the photoresist film was dissolved with dimethylformamide. Annealing of the contact and removal of organic matter residues from the surface was carried out in a low vacuum at 200 °C for 5 min.

The homogenous arrays of highly oriented ZnO nanorods of 30–500 nm in diameter and 10–15 μm length (Fig. 4) were obtained by controlling the conditions of the nanorods growth using carbothermal technique.

5. Results and Discussion

The Au/ZnO nanorods/ZnO film/Au/SiO_2/Si structure has diode U–I characteristic as shown in Fig. 5. It is seen that the U–I characteristic is not symmetrical, which means that only one barrier between Au and the ZnO was formed in the structure.

In addition, experiments carried out to study the formation of the Schottky barrier at the Au/ZnO interface proved that the barrier occurs at the boundary of the lower Au contact and deposited ZnO film.

Deposition of the ZnO film was conducted on a substrate already heated to 500 °C, so the concentration of the adsorbed molecules on the Au surface was much lower. This has a positive effect on the Schottky barrier Au/ZnO formation.

For nanorods obtained by carbothermal technique on the Au surface only two sharply defined reflexes to 34.5° and 38.3° were observed, which correspond to the crystallographic orientations (0 0 2) and (1 1 1) of zinc oxide and Au, respectively [Fig. 6(a)]. Thus, it can be argued that the nanorods of zinc oxide obtained by carbothermal synthesis were oriented only along the *c*-axis normal to the substrate. The full width half maximum (FWHM) of the rocking curve of the (0002) peak is very narrow, about 0.23°, indicating the small angular dispersion of the crystallites around the *c*-axis and excellent ZnO crystal formation.[19]

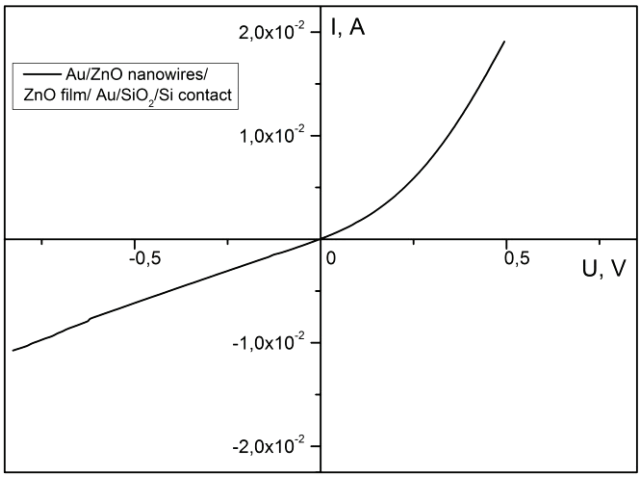

Fig. 5. The current–voltage characteristic of the Au/ZnO nanorods/ZnO film/Au/SiO_2/Si structure. Nanorods were obtained by carbothermal technique.

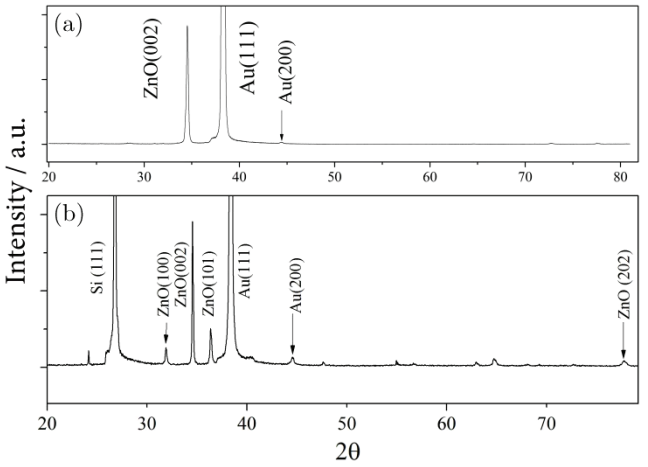

Fig. 6. XRD of ZnO nanorods grown using carbothermal (a) and electrochemical methods (b).

XRD study of nanorods obtained by electrochemical method revealed peaks near 31.7°, 34.4° and 36.2°, corresponding to (1 0 0), (0 0 2) and (1 0 1) crystallographic orientations of wurtzite ZnO structure [Fig. 6(b)]. The nanorods have preferable orientation with *c*-axis normal to substrate.

The PL study of the ZnO nanorods grown by carbothermal technique shows blue exciton PL peak at 382 nm and a broad band of green/red emission at 450–800 nm related to structural point defects of ZnO as it is shown in Fig. 7. The high amount of defects was caused by the high temperature of 1000 °C used for synthesis. The defect related band consists of several bands supposedly centered near 490, 518, 575, 607 and 632–650 nm (2.53, 2.39, 2.15, 2.04 and 1.96–1.9 eV). The bands near 2.53, 2.39 eV were earlier assigned as oxygen and zinc atom vacancies V_O and V_{Zn}.[20] The band of 2.39 eV is sometimes also attributed to O_i and O_{Zn} point defects.[21] The red band near 1.96–1.9 eV was observed before in Refs. 22 and 23, whereas their origin is still under debate. PL of the spectra of the ZnO nanorods obtained by electrochemical method shows only a broad band of orange-red emission centered at 632–650 nm related to structural defects.

Raman spectrum of nanorods, obtained by electrochemical deposition on Au electrode, is shown in Fig. 8(a).

The spectra reveal peaks near 99 cm^{-1}, 438 cm^{-1} and 572 cm^{-1}, corresponding to E_2^{low}, E_2^{high} and A_1(LO) lattice vibrations of not stressed ZnO wurtzite structure.[24,25] The mode at 335 cm^{-1} corresponds to $E_2^{high} - E_2^{low}$ two-phonon process. An additional multi-phonon Raman scattering processes observed as broad bands at 335–438 cm^{-1} and 438–572 cm^{-1} evidence the relaxation of the selection rules induced by point defects.

Raman spectrum of ZnO-rods/Au revealed only two peaks corresponding to E_2^{low} and E_2^{high} phonon modes of wurtzite ZnO at 98 cm^{-1} and 436 cm^{-1} as shown in Fig. 8(b).

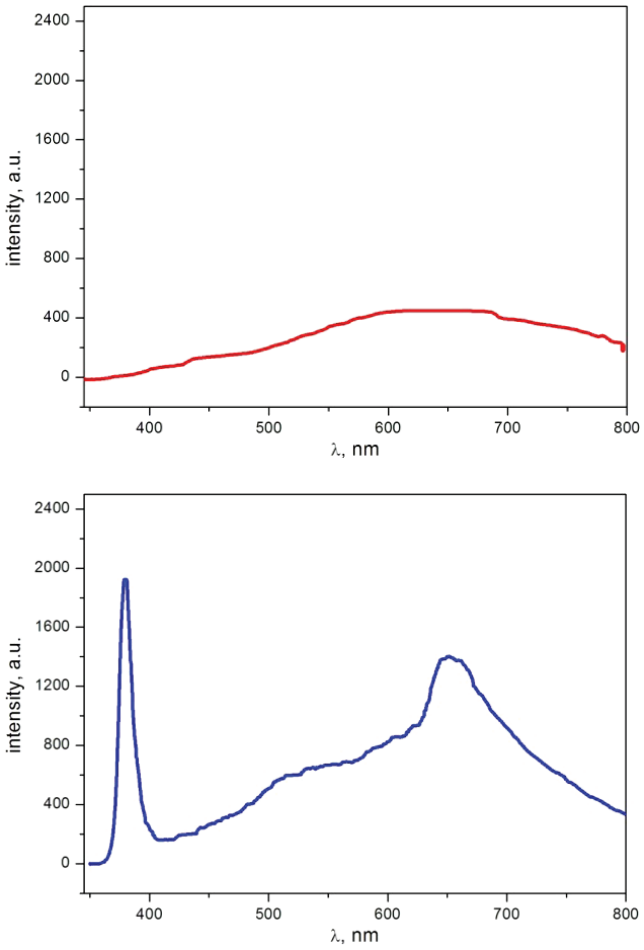

Fig. 7. (Color online) PL spectrum of nanorods obtained by electrochemical deposition technique (red) and carbothermal technique (blue).

The spectra had high noise level induced by high reflectivity of Au electrode. Typically the A_1(LO) phonon band becomes stronger only in the highly crystalline ZnO.[26]

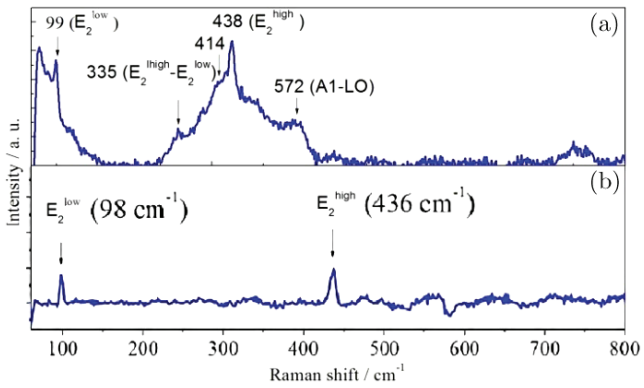

Fig. 8. The Raman spectrum of the nanorods obtained by electrochemical method (a) and carbothermal technique (b).

The hydrothermal synthesis did not allow the growth of a dense array of vertically oriented ZnO nanorods. It was not possible to grow nanorods with the required geometrical parameters by changing the synthesis temperature, exposure time, parameters of applying the seed layer, and changing the concentration of the components. Therefore, we presented the best synthesis parameters and a SEM image of the most successful sample [Fig. 2(a)]. Further, we did not study nanorods obtained by the method of hydrothermal synthesis. Nanorods obtained by electrochemical and carbothermal methods, on the contrary, were well oriented along the axis perpendicular to the plane of the substrate [Figs. 2(b) and 4]. A small spread in the length of the rods allows the top contact to be well positioned according to the developed lift-off technique. As a result, it was possible to minimize the drift of the contact along the surface of the rods during dissolution of the photoresist film and to clearly position the contact pad in the required place. X-ray spectra confirm the previous statements for a large area of the sample since the field of view of the SEM is extremely small and does not allow the analysis of the sample as a whole (Fig. 6). These spectra revealed that the ZnO nanorods obtained by the method of carbothermal synthesis are more crystalline than those obtained using the electrochemical method. This is explained by the large number of structural defects, which we can qualitatively estimate from the luminescence spectra (Fig. 7). In the spectra of nanorods obtained by the carbothermal technique, we see a wide defect "green region", which is most likely associated with a high synthesis temperature. In our previous study, we showed that it is possible to reduce the synthesis temperature without affecting the structure of the rods to reduce the concentration of point defects.[27,28] All of the above indicates that the carbothermal technique is the most flexible tool for producing ZnO nanorods with controlled defectiveness, which is a very important condition for their applications in micro- and nanoelectronics. Also, the considered methods make it possible to obtain well-oriented and dense arrays of nanorods, which is very important in the formation of the upper ohmic contact (Fig. 4). These results allow one to use ZnO nanorods for detecting gases, organic molecules, optical radiation, etc. by changing the mass of one of the resonator contact, or obtaining microbalanced and bulk resonators, the active element of which will be an array of ZnO nanorods.

6. Conclusion

ZnO nanorods were obtained by the methods of carbothermal, electrochemical, and hydrothermal synthesis. Carbothermal synthesis makes it possible to obtain the most crystallinely perfect, homogeneous, and dense arrays of nanorods and control the concentration of point defects by changing the synthesis parameters over a wide range. Due to the piezoelectric properties of zinc oxide, this method is well suited for obtaining of microbalanced and bulk resonators with pronounced photo and gas sensitivity. This is possible due to the

developed technique for applying the upper ohmic contact to zinc oxide nanorods. The electrochemical synthesis is well suited for the synthesis of ZnO nanorods on the surface of resonator electrodes. In this case, the adsorbed molecules will change the mass of the electrodes. This fact allows to evaluating the presence and concentration of adsorbed substances in the media by the shift of the resonance frequency. It should also be noted that the temperature of electrochemical synthesis is 70 °C, which is well below the Curie point for most common piezoelectric materials. Whereas the use of carbothermal synthesis for the growth of nanorods on the contacts of the resonator is only for piezoelectrics with a Curie point much higher than 1000 °C. Among the further priorities to expand the current study, we plan to use methods of mathematical modeling[29–31] to achieve more predictable and enhanced strength properties of the multilayered structures obtained.

Acknowledgments

Financial support was provided by the Russian Foundation for Basic Research, project 20-07-00637 A.

References

[1]L. L. Ke, Y. S. Wang and Z. D. Wang, Nonlinear vibration of the piezoelectric nanobeams based on the nonlocal theory, *Compos. Struct.* **94**(6), 2038 (2012).

[2]C. Liu, L. L. Ke, Y. S. Wang, J. Yang and S. Kitipornchai, Thermo-electro-mechanical vibration of piezoelectric nanoplates based on the nonlocal theory, *Compos. Struct.* **106**, 167 (2013).

[3]V. A. Eremeyev, On effective properties of materials at the nano- and microscales considering surface effects, *Acta Mech.* **227**(1), 29 (2016).

[4]Z. Yan, X. Y. Zhou, G. K. H. Pang, T. Zhang, W. L. Liu, J. G. Cheng and Y. Wang, ZnO-based film bulk acoustic resonator for high sensitivity biosensor applications, *Appl. Phys. Lett.* **90**(14), 143503 (2007).

[5]X. Bian, H. Jin, X. Wang, S. Dong, G. Chen, J. K. Luo and B. Qi, UV sensing using film bulk acoustic resonators based on Au/n-ZnO/piezoelectric-ZnO/Al structure, *Sci. Rep.* **5**(1), 1 (2015).

[6]Z. Wang, X. Qiu, S. J. Chen, W. Pang, H. Zhang, J. Shi and H. Yu, ZnO based film bulk acoustic resonator as infrared sensor, *Thin Solid Films* **519**(18), 6144 (2011).

[7]S. Kiruthika, S. Singh and G. U. Kulkarni, Large area transparent ZnO photodetectors with Au wire network electrodes. *RSC Adv.* **6**(50), 44668 (2016).

[8]Z. Yan and X. J. Zhou, Simulation of ZnO based film bulk acoustic resonator by modified Butterworth-Van Dyke model, In *Proceedings of the 2010 Symposium on Piezoelectricity, Acoustic Waves and Device Applications*, pp. 491–496 (2010). doi: 10.1109/SPAWDA.2010.5744362.

[9]B. A. Buchine, W. L. Hughes, F. L. Degertekin and Z. L. Wang, Bulk acoustic resonator based on piezoelectric ZnO belts, *Nano Lett.* **6**(6), 1155 (2006).

[10]D. Yang, W. Song, H. Chen, Y. Li, Z. Zhang, J. Xu and Y. Qiu, Enhanced performance of ZnO piezoelectric nanogenerators by using Au-coated nanowire arrays as top electrode, *Phys. Stat. Solidi (A)* **212**(9), 2001 (2015).

[11]P. I. Reyes, Z. Zhang, H. Chen, Z. Duan, J. Zhong, G. Saraf and N. N. Boustany, A ZnO nanostructure-based quartz crystal microbalance device for biochemical sensing, *IEEE Sens. J.* **9**(10), 1302 (2009).

[12]N. Van Quy, V. A. Minh, N. Van Luan, V. N. Hung and N. Van Hieu, Gas sensing properties at room temperature of a quartz crystal microbalance coated with ZnO nanorods, *Sens. Actuators B Chem.* **153**(1), 188 (2011).

[13]M. Willander, L. L. Yang, A. Wadeasa, S. U. Ali, M. H. Asif, Q. X. Zhao and O. Nur, Zinc oxide nanowires: controlled low temperature growth and some electrochemical and optical nano-devices, *J. Mater. Chem.* **19**(7), 1006 (2009).

[14]J. Y. Li, X. L. Chen, H. Li, M. He and Z. Y. Qiao, Fabrication of zinc oxide nanorods, *J. Cryst. Growth* **233**(1–2), 5 (2001).

[15]E. Sadyrin, M. Swain, B. Mitrin, I. Rzhepakovsky, A. Nikolaev, V. Irkha, D. Yogina, N. Lyanguzov, S. Maksyukov and S. Aizikovich, Characterization of enamel and dentine about a white spot lesion: Mechanical properties, mineral density, microstructure and molecular composition, *Nanomaterials* **10**(9), 1889 (2020).

[16]E. V. Sadyrin, B. I. Mitrin, L. I. Krenev, A. L. Nikolaev and S. M. Aizikovich, Evaluation of mechanical properties of the two-layer coating using nanoindentation and mathematical modeling, *Int. Conf. Physics and Mechanics of New Materials and Their Applications* (Springer, Cham, 2017), pp. 495–502.

[17]D. A. Zhilin, V. I. Pushkariov, L. A. Nikolaev, E. M. Kaidashev, N. V. Lyanguzov and V. E. Kaydashev, Photoelectric properties of metal-semiconductor-metall structure based on ZnO nanorods designed thermal evaporation and carbothermal methods, *Adv. Mater. Stud. Appl.* ISBN: 978-1-63463-749-7, Chapter 5, pp. 57–64 (2015).

[18]V. I. Pushkariov, A. L. Nikolaev and E. M. Kaidashev, Synthesis and characterization of ZnO nanorods obtained by catalyst-free thermal technique, *J. Phys. Conf. Ser.* **541**, 012031 (2014).

[19]X. L. He, L. Garcia-Gancedo, P. C. Jin, J. Zhou, W. B. Wang, S. R. Dong and W. I. Milne, Film bulk acoustic resonator pressure sensor with self temperature reference, *J. Micromech. Microeng.* **22**(12), 125005 (2012).

[20]T. M. Børseth, B. G. Svensson, A. Y. Kuznetsov, P. Klason, Q. X. Zhao and M. Willander, Identification of oxygen and zinc vacancy optical signals in ZnO, *Appl. Phys. Lett.* **89**(26), 262112 (2006).

[21]A. F. Kohan, G. Ceder, D. Morgan and C. G. Van de Walle, First-principles study of native point defects in ZnO, *Phys. Rev. B* **61**(22), 15019 (2000).

[22]S. A. Studenikin, N. Golego and M. Cocivera, Fabrication of green and orange photoluminescent, undoped ZnO films using spray pyrolysis, *J. Appl. Phys.* **84**(4), 2287 (1998).

[23]R. E. Marotti, J. A. Badán, E. Quagliata and E. A. Dalchiele, Red photoluminescence and band edge shift from ZnO thin films, *Physica B Condens. Matter* **398**(2), 337 (2007).

[24]C. A. Arguello, D. L. Rousseau and S. D. S. Porto, First-order Raman effect in wurtzite-type crystals, *Phys. Rev.* **181**(3), 1351 (1969).

[25]O. Lupan, L. Chow, G. Chai, B. Roldan, A. Naitabdi, A. Schulte and H. Heinrich, Nanofabrication and characterization of ZnO nanorod arrays and branched microrods by aqueous solution route and rapid thermal processing, *Mater. Sci. Eng. B* **145**(1–3), 57 (2007).

[26]A. L. Nikolaev, E. M. Kaidashev and A. S. Kamencev, Morphology and photoluminescence of zinc oxide nanorods obtained by carbothermal synthesis at different temperatures, *Adv. Mater.* **224**, 103, (2019).

[27]V. I. Pushkariov, A. L. Nikolaev and E. M. Kaidashev, Influence of Zn vapor supersaturation on morphology and optical properties of

ZnO nanorods grown by CVD technique, *Adv. Mater. Stud. Appl.* ISBN: 978-1-63463-749-7, Chapter 4, pp. 51–56 (2015).
[28]A. L. Nikolaev, B. I. Mitrin, E. V. Sadyrin, V. B. Zelentsov, A. R. Aguiar and S. M. Aizikovich, Mechanical properties of microposit S1813 thin layers, in *Modeling, Synthesis and Fracture of Advanced Materials for Industrial and Medical Applications*. (Springer, Cham, 2020), pp. 137–146.
[29]E. V. Sadyrin, A. S. Vasiliev, S. S. Volkov, B. I. Mitrin and S. M. Aizikovich, Simplified analytical solution of the contact problem on indentation of a coated half-space by a spherical punch, *WIT Trans. Eng. Sci*. **122**, 209 (2019).
[30]V. B. Zelentsov, E. V. Sadyrin, A. G. Sukiyazov and N. Y. Shubchinskaya, On a method for determination of Poisson's ratio and Young modulus of a material, *MATEC Web of Conf.*, Vol. 226 (EDP Sciences, 2018), p. 03027.
[31]L. I. Krenev, S. S. Volkov, E. V. Sadyrin and S. A. Chizhik, Mechanical material tests by the nanoindentation method at various indenter and specimen temperatures, *J. Eng. Phys. Thermophys.* **91**(3), 594 (2018).